Grid-connected inverters per-unit Dynamic Phasor modelling, simulation and control

Álvaro A. Volpato * Luís F. C. Alberto **

* Department of Electrical and Computer Engineering, São Carlos
School of Engineering, University of São Paulo
(alvaro.volpato@usp.br)
** Department of Electrical and Computer Engineering, São Carlos
School of Engineering, University of São Paulo (lfcalberto@usp.br)

Abstract: Given the increasing penetration of photovoltaic and battery-powered systems in macro and microgrids, efficient and reliable modelling of the inverters for studying the stability of such systems is paramount. In the current academia standard, generic inverter models, which do not coherently represent inverter behavior nor consider inverter topology and filter, are used – undermining the presented results. This paper presents a thorough and comprehensive per-unit modelling of inverter systems based on a strong mathematical foundation. This modelling is compatible with Equivalent Phasor techniques, generally used for synchronous machines, which allow simulation and study of stability of mixed systems where both technologies are present.

Keywords: Modelling, Inverter, Simulation, Dynamic.

1. INTRODUCTION

Due to the high penetration of wind and photovoltaic-powered systems into electric grids, renewable power has become a major industry and academic field in the current setting, making imperative the development of precise and reliable models of the components of such systems. For instance, a photovoltaic system is generally comprised of three main parts, each of which with very particular dynamics and characteristics: the PV panels, configured in an array, which provide electrical power; a DC-DC converter regulated by a Maximum Power Point Tracking logic which ensures the array works at a maximum power condition; and an inverter, or DC-AC converter, which transforms the DC power fed from the DC-DC converter to an AC power which is then passed on to the grid. This scheme is represented in figure 1.

Inverter topologies are common to wind, battery and photovoltaic-powered systems, the only differentiation being control strategies and objectives. The commonplace inverter control is aimed at regulating its output power angle to a setpoint, most commonly to unitary power factor – that is, the inverter outputs active power only – by adjusting the trigger angle of the electronic switches (most commonly IGBTs) in the switching bridge, that modulates the DC power creating an alternating wave. Thence a filter (most commonly LCL or LC) is used to adjust the alternating wave from the switching bridge, ideally removing high-order harmonics and outputting a pure-sine wave (Kulasza (2014)).

Not unbeknownst to engineers and academics, both bridge and filter topologies affect inverter performance and dynamics; however, in most stability or power researches, authors use standard models (Wu et al. (2016)) which do not translate those dynamics nor comprehensively model filter or switching effects (Kotian and Shubhanga (2016)). These models are known to sufficiently resemble real-world behavior in a very strict set of conditions — specially static behavior; however, as the stability studies get more sophisticated, inverter dynamics play a big role in the end result and conclusion.

Also, the used models generally do not conform to the modelling standards of Electric Power Systems. Researchers have, for over 50 years, used very known and understood models for Synchronous Machines which are applied in very particular ways so as to make simulation numerically faster, more stable, and its results easier to interpret and analyse. The Equivalent Phasor Modelling of such machines, generally obtained by means of Park Transformation, which supposes the grid in a static sinusoidal state, yields currents and voltages in their equivalent phasorial forms and is dominant over Electromechanical Transient models, specially in stability researches. Another academic standard is the per-unit modelling, which allows engineers to analyse systems based on normalized quantities, giving fast insights, for instance, at what percentage of rated values the system operates at or if any operation limit condition was violated. In this regard, models for converter-based systems must be compatible with those already in use for Synchronous Machines to make possible their integration in the same framework, allowing the study of mixed grids where both technologies — converter-based generators and machine-based generators — are present.
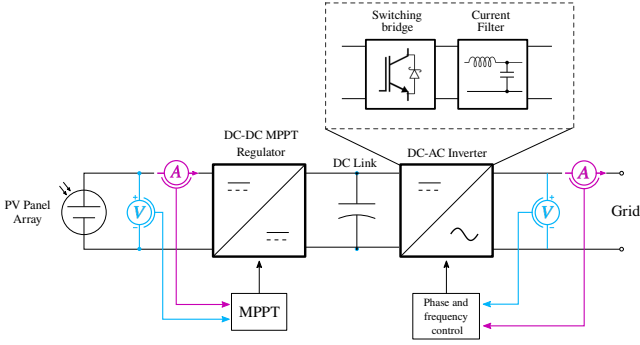
Figure 1. Generic block diagram representation of a pvo-tovoltaic generator.

Currently, however, there is no widespred inverter model that has both phasorial and per-unit characteristics. Hence it is paramount to not only have deep knowledge and complete understanding of the inverter models but also to have inverter models that are compatible with the already standardized machine models – phasorial and per-unit being their main characteristics. This paper then aims at presenting a modelling technique known as Dynamic Phasor Modelling, which is based on the Fourier Transform for Differential Equations, that can be used with any converter topology to yield per-unit and phasorial modelling of that particular topology. Thence, particular topologies of inverting bridge and filter are adopted to make a case study and simulations are presented.

2. DYNAMIC PHASORS

2.1 Fundamentals

The premise of Dynamic Phasor Modelling (DPM) is that any signal $x(t)$ can be approximated to arbitrary precision by a Fourier Series, like in (1), such that the Fourier Coefficients are time-variant (Sanders et al. (1991)). This approach consists of, at every time t, executing the Fourier Analysis of x in a window $(t - T, t]$; this window "slides" over time such that each time instant yields different coefficients.

Theorem 1. (Dynamic Phasor Analysis). Consider a signal $x(t) : \mathbb{R} \to \mathbb{R}$, T a window period and $\omega = 2\pi T^{-1}$ the window angular frequency. Then, for every τ in $(t - T, t]$,

$$x(\tau) = \sum_{k \in \mathbb{Z}} \langle x \rangle_k(t) \, e^{jk\omega\tau} \tag{1}$$

where $\langle x \rangle_k(t) : \mathbb{R} \to \mathbb{C}$ is a time-dependant coefficient known as k-th harmonic; the first harmonic is also known as *fundamental*. Harmonics are calculated as

$$\langle x \rangle_k(t) = \frac{1}{T} \int_{t-T}^{t} x(\lambda) \, e^{-jk\omega\lambda} d\lambda \tag{2}$$

Proof. For every instant t, define the periodic expansion $y_t(\tau)$ of $x(t)$, such that

$$y_t(\tau) = x(t - T + \tau) \, \forall \tau \in (0, T] \tag{3}$$

Thence the Fourier Series of y_t yields

$$y_t(\tau) = \sum_{k \in \mathbb{Z}} \langle y_t \rangle_k \, e^{jk\omega\tau} \tag{4}$$

where

$$\langle y_t \rangle_k = \frac{1}{T} \int_{0}^{T} y_t(\lambda) \, e^{-jk\omega\lambda} d\lambda \tag{5}$$

Making a little agebraic manipulation,

$$y_t(\tau) = \sum_{k \in \mathbb{Z}} \left[\langle y_t \rangle_k \, e^{-jk\omega(t-T)} \right] e^{jk\omega(t-T+\tau)} \tag{6}$$

$$\langle y_t \rangle_k \, e^{-jk\omega(t-T)} = \frac{1}{T} \int_{0}^{T} y_t(\lambda) \, e^{-jk\omega(t-T+\lambda)} d\lambda \tag{7}$$

Results are immediate once substitution (3) is made and $\langle x \rangle_k(t) = \langle y_t \rangle_k \, e^{-jk\omega(t-T)}$ is adopted. □

This approach is known as Dynamic Phasor Modelling because the harmonics, being complex values, represent a piece of the spectrum of x in a given instant, and hence are time-variant, that is, dynamic.

2.2 Dynamic phasors in Electric Power Systems

Most stability studies will admit that the grid is at its stationary sinusoidal behavior; this assumption allows the complexification of any sinusoid $s(t) = \Lambda_0 \cos(\omega t + \theta_0)$ into a phasor $S(t) = \Lambda_0 e^{j\theta_0}$. This is justified because $s(t)$ is a stable solution to any ordinary differential equation with sinusoidal forcing – which is the reason why signal $s(t)$ has a frequency spectrum of a single harmonic on frequency ω, with amplitude Λ_0 and phase θ_0. However, in Electrical Power System studies, the main concern are signals of the sinusoidal form which magnitude and phase are time-variant.

$$x(t) = \Lambda(t) \cos[\omega t + \theta(t)] \tag{8}$$

Contrary to $s(t)$, signal (8) does not admit a phasorial representation in priciple: of course, when Λ and θ are constant, the result is immediate but, when these quantities are time-variant, $x(t)$ will not present a single harmonic and hence does not admit phasorial representation. In this context, a natural question would be if signal (8) can be represented by an extended idea of phasor, phasor variant in time; the intuitive candidate would be

$$X(t) = \Lambda(t) e^{j\theta(t)} \tag{9}$$

Under some circumstances, however, $x(t)$ can be approximated by a sinusoid and admit an approximate phasorial representation. For instance, if we admit that the absolute value $\Lambda(t)$ and phase $\theta(t)$ of $x(t)$ are arbitrarily "slow" compared to x itself, that is, they have a frequency

spectrum arbitrarily below ω, then $x(t)$ can be arbitrarily approximated by a sinusoid and the fundamental harmonic will be dominant over its higher-order counterparts; this proves the sought approximation.

Definition 2. (Bernstein's equality). (Zayed (2008)) The **bandwidth** of a signal $z(t) : \mathbb{R} \to \mathbb{R}$ in interval $I \subset \mathbb{R}$ is defined as

$$\omega_z = \frac{1}{\sup\limits_{t \in I} |z(t)|} \sup\limits_{t \in I} \left| \frac{dz(t)}{dt} \right| \tag{10}$$

Lemma 3. With Λ and θ as in equation (8), define

$$\varepsilon_\Lambda(t) = \Lambda(t) - \Lambda_0(t) \tag{11}$$

$$\varepsilon_\theta(t) = \theta(t) - \theta_0(t) \tag{12}$$

Where $\Lambda_0(t)$ and $\theta_0(t)$ are the mean values of those signals in the window $(t - T, t]$. Define $\omega_\Lambda(t)$ and $\omega_\theta(t)$ as the bandwidth of signals Λ and θ in $(t - T, T]$. Then functions ε_Λ and ε_θ converge uniformly to the null function as ω_Λ and ω_θ tend to zero.

Theorem 4. (Sinusoidal approximation). The Fourier Coefficients of $x(t)$ as defined in (8) get arbitrarily close to those of the sinusoidal signal $s(t) = \Lambda_0 \cos(\omega t + \theta_0)$ as ω_Λ and ω_θ tend to zero.

Proof. Adopt $x(t)$ as in (8) and ε_Λ and ε_θ as defined in the lemma. By the results of Theorem 1, $x(t)$ coefficients can be written as

$$\langle x \rangle_n(t) = \frac{1}{T} \int_{t-T}^{t} (\Lambda_0 + \varepsilon_\Lambda) \cos(\omega\lambda + \theta_0 + \varepsilon_\theta) e^{-jk\omega\lambda} d\lambda \tag{13}$$

By developing this equation one obtains

$$\langle x \rangle_n - \langle s \rangle_n =$$

$$\frac{1}{T} \int_{t-T}^{T} \{ \varepsilon_\Lambda \cos(\omega\lambda + \theta_0) \cos(\varepsilon_\theta) + \Lambda_0 \cos(\omega\lambda + \theta_0) [\cos(\varepsilon_\theta) - 1] +$$

$$-\Lambda_0 \sin(\omega\lambda + \theta_0) \sin(\varepsilon_\theta) - \varepsilon_\Lambda \sin(\omega\lambda + \theta_0) \sin(\varepsilon_\theta) \} e^{-jk\omega\lambda} d\lambda \tag{14}$$

Adopting the Triangular Modular Inequality for complex integrals,

$$|\langle x \rangle_k - \langle s \rangle_k| \leq$$

$$|\varepsilon_\Lambda| + 2\sin^2(\varepsilon_\theta) |\Lambda_0| + |\Lambda_0 \sin(\varepsilon_\theta)| + |\varepsilon_\Lambda \sin(\varepsilon_\theta)| \tag{15}$$

Let $\omega_\mathrm{m} = \max(\omega_\alpha, \omega_\beta)$. Applying lemma 3 then yields

$$\lim_{\omega_\mathrm{m} \to 0} \langle x \rangle_k = \langle s \rangle_k \tag{16}$$

Since Lemma 3 proves ε_Λ and ε_θ converge uniformly, so does $\langle x \rangle_k$ converge uniformly. $\square$

Ultimately, this means that the signal $x(t)$ can be represented by an equivalent phasor $X(t) = \alpha(t)e^{j\beta(t)} : \mathbb{R} \to \mathbb{C}$, where $\alpha(t)$ and $\beta(t)$ have "slow" dynamics and can be approximated by their mean values at the window $(t - T, t]$.

Some interesting properties of the Dynamic Phasor Analysis are directly inherited from Fourier Analysis, such as:

$$\textbf{Linearity} : \langle x + y \rangle_k(t) = \langle x \rangle_k(t) + \langle y \rangle_k(t) \tag{17}$$

$$\textbf{Convolution} : \langle xy \rangle_k(t) = \sum_{n \in \mathbb{Z}} \langle x \rangle_k(t) \langle y \rangle_{n-k}(t) \tag{18}$$

$$\textbf{Uniqueness} : (\forall k \in \mathbb{Z}) (\langle x \rangle_k(t) = \langle y \rangle_k(t)) \Leftrightarrow$$

$$\Leftrightarrow (\forall t \in \mathbb{R}) (x(t) = y(t)) \tag{19}$$

The most important of them, however, is the ability to convert time-defined differential equations into phasor-defined equations:

$$\left\langle \frac{dx}{dt} \right\rangle_k = \frac{d \langle x \rangle_k}{dt} + jk\omega \langle x \rangle_k \tag{20}$$

3. INVERTER DPM MODELLING AND CONTROL

As stated in the introduction, the commonplace inverter topologies are comprised of two subsystems: a switching bridge that modulates the DC input voltage into an alternating waveform, and a current filter that purifies the wave to near-pure sinusoidal current, removing high-order harmonics.

As a case study, the inverter in figure 2 is used. It is comprised of a single-stage, full-switching bridge (which outputs an alternating voltage $v_1(t)$) with LCL filter which outputs a sine wave $v_2(t)$; the DC power is fed from a constant voltage source V_S with equivalent series resistance R_S. The system is attached to an Infinite Bus, representing the macrogrid, through a line of impedance Z_L.

The system is equipped with a PI controller that measures output power angle $\Delta\phi$ and adjusts it to a setpoint $\Delta\phi_R$, generally zero – aiming at unitary power factor. This control is done by adjusting the electronics switch trigger time, modulating the phase of voltage $v_1(t)$. Also, suppose base voltage, power and frequency values V_b, ω_b and S_b are already adopted.

Both subsystems are modelled independently and make use of the Dynamic Phasor technique presented last section. All components are supposed ideal – no losses or parasitic effects are considered. Aditionally, high-order harmonics are purposefully neglected and only fundamental harmonics are considered under the assumption that the current filter deployed reduces harmonics substantially.

3.1 Current filter modelling

The current filters generally used in inverters are composed of a specific combination of inductances and capacitances;
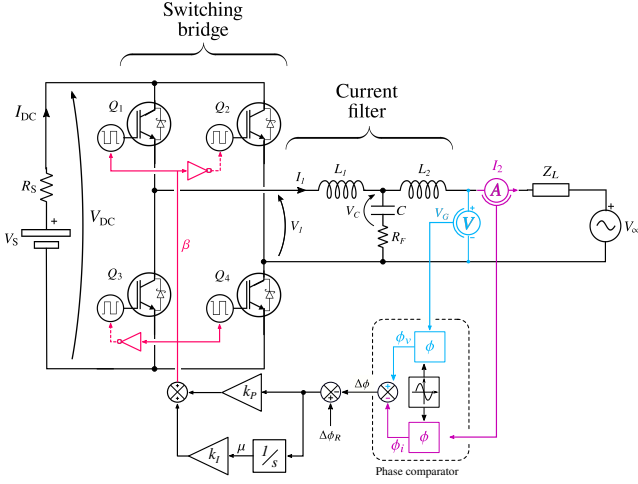
Figure 2. Inverter topology used in DPM case study.

each topology has advantages and disadvantages – which in general fall into a tradeoff between performance and losses (Kahlane et al. (2014)). The capacitor and inductor time equations can easily be translated into phasorial differential equations through (20); for instance, take the capacitor current-voltage equation

$$i = C \frac{dv}{dt} \tag{21}$$

Considering a voltage signal like (8) is applied, then Dynamic Phasor analysis to both sides of equation (21) yields

$$\langle i \rangle_k = C \left[\frac{d \langle v \rangle_k}{dt} + jk\omega \langle v \rangle_k \right] \tag{22}$$

Interestingly, when the applied voltage does not vary in phase nor modulus, then this equation becomes $\langle i \rangle_k = jCk\omega \langle v \rangle_k$, which is the common capacitive impedance equation; in this regard, Dynamic Phasor Modelling can be seen as a natural expansion of impedance equations when the considered phasors have changing characteristics.

Under the supposition that high-order harmonics are negligible compared to fundamental harmonics, variables in lowercase represent their time signals and uppercase their first-order phasorial equivalents. Writing the time equations of the filter in figure 2,

$$\begin{cases} v_1 - v_C - R_F (i_1 - i_2) = L_1 \dot{i}_1 \\ v_C + R_F (i_1 - i_2) - v_2 = L_2 \dot{i}_2 \\ i_1 - i_2 = C \dot{v}_C \end{cases} \tag{23}$$

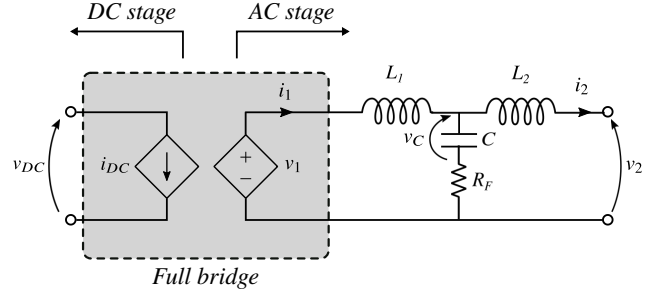Applying (8) for the fundamental harmonic,

Figure 3. Inverter switching bridge simplified modelling.

$$\begin{cases} V_1 - V_C - R_F (I_1 - I_2) = L_1 \left(\frac{dI_1}{dt} + j\omega I_1 \right) \\ V_C + R_F (I_1 - I_2) - V_2 = L_2 \left(\frac{dI_2}{dt} + j\omega I_2 \right) \\ I_1 - I_2 = C \left(\frac{dV_C}{dt} + j\omega V_C \right) \end{cases} \tag{24}$$

It must be noted that the values in this system are complex-valued – since they are the harmonics of the time signals – and as such this system yields six real differential equations. It is also noteworthy that if the complex axis is congruent to the d-q axis, then the real and imaginary parts of each phasor coincide with their direct and quadrature components. In other words, when system (24) is separated into imaginary and real parts, it yields a sixth-order differential system on variables V_1^d, V_1^q, V_2^d, V_2^q, I_1^d, I_1^q, V_C^d, V_C^q.

Having the base voltage, current and impedance values V_b, I_b and Z_b in hand, divide the first and second equations of (24) by V_b and the third by I_b. Adopt $\omega L_1 = x_1$, $\omega L_2 = x_2$, $\omega C = y_C$, all measured in per-unit values. Also adopt $L_1 Z_b^{-1} = \tau_1$, $L_2 Z_b^{-1} = \tau_2$ and $C Z_b = \kappa$ as time constants related to the filter dynamics. Using these equalities, then (24) can be re-written in a more familiar manner, where all variables are now designated in their per-unit values:

$$\begin{cases} \frac{dI_1}{dt} = \frac{V_1 - V_C - R_F (I_1 - I_2) - jx_1 I_1}{\tau_1} \\ \frac{dI_2}{dt} = \frac{V_C + R_F (I_1 - I_2) - V_2 - jx_2 I_2}{\tau_2} \\ \frac{dV_C}{dt} = \frac{I_1 - I_2 - jy_C V_C}{\kappa} \end{cases} \tag{25}$$

3.2 Switching bridge modelling

The inverter switching bridge is modelled as a two-part system with a DC and an AC stage, as in figure 3.

The two stages are related by a power flow equation: in the average of a cycle, the mean DC input power and RMS AC output power of the bridge must be the same:

$$\mathbf{Re}\,(V_1 I_1^*) = V_1^d I_1^d + V_1^q I_1^q = I_{\mathrm{DC}} V_{\mathrm{DC}} \tag{26}$$

Dividing equation (26) by the base power value S_b will transform the variables in their per-unit values. Furthermore, the bridge topology dictates how the input DC
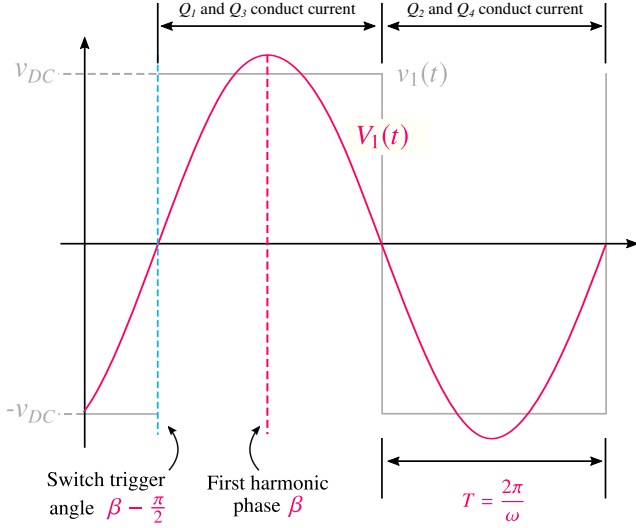
Figure 4. Time diagram showing the relation between phasor V_1, time signal v_1 and DC voltage v_{DC}.

voltage is modulated; particularly for the system in figure 2, the output wave $v_1(t)$ is a square wave which amplitude is v_{DC} and phase β is fed from the controller, as depicted in figure 4.

Since v_1 is a square wave, by applying Dynamic Phasor modelling one obtains

$$v_1(t) = \frac{4v_{\mathrm{DC}}}{\pi} \sum_{n \in 2\mathbb{N}+1} \frac{1}{n} e^{j(n\omega t + n\beta)} \Rightarrow$$

$$\Rightarrow \langle v_1 \rangle_n (t) = \frac{4v_{\mathrm{DC}}}{n\pi} e^{jn\beta(t)} \quad (27)$$

Then again, disconsidering higher-order harmonics due to filter action, one can write

$$V_1(t) = \frac{4V_{\mathrm{DC}}}{\pi} e^{j\beta(t)} \Rightarrow \begin{cases} V_1^d = \dfrac{4V_{\mathrm{DC}}}{\pi} \cos(\beta) \\ \\ V_1^q = \dfrac{4V_{\mathrm{DC}}}{\pi} \sin(\beta) \end{cases} \quad (28)$$

3.3 Power factor control

As aforementioned, the system of figure 2 has a PI controller that modulates the switch trigger angle β, which translates into the phase of bridge output voltage V_1, to adjust the output power angle to a setpoint. The phase comparator block – built with fast PLLs which operate in the MHz range – is considered fast such that its dynamics are negligible. Hence, the control equations resulting from the PI controller are

$$\begin{cases} \Delta\phi = \arcsin\left(\dfrac{V_2^q I_2^d - V_2^d I_2^q}{|V_2||I_2|}\right) \\ \\ \dot{\gamma} = \Delta\phi - \Delta\phi_R \\ \\ \beta = k_P\left(\Delta\phi - \Delta\phi_R\right) + k_I\gamma \end{cases} \quad (29)$$

It is important to note that the power factor control can use only measurements local to the inverter; it follows that β is the angle of V_1 measured when V_2, the inverter output voltage, is the phase reference. If no frequency control is used, as is the case in this example, system (29) sufficiently describe the angle control needed. However, if some form of frequency control is deployed, then the angle of V_2 is not stationary and an additional term for an angle deviation caused by frequency control must be considered.

4. RESULTS

Equations (25),(26), (28) and (29) then form an agebraic-differential system that is used to simulate it dynamically. The model parameters used in the simulation are described in table 2, and the initial conditions in table 1.

Simulation was conducted with a disturbance in the power angle reference, which starts at $\Delta\phi_R = 0$ in t = 0 and steps to 0.1 radians at t = 5 ms. Simulation results are shown in figure 5.

Table 1. Initial conditions for the simulation of the standalone inverter.

Param.	Description	Value (p.u.)
S_2	Output complex power	$1e^{j0}$
V_∞	Infinite bus voltage	$0.9950e^{-j0.1007}$
V_2	Output voltage	$1e^{j0}$
I_2	Output current	$1e^{j0}$
V_1	Bridge output voltage	$1.023e^{j0.2201}$
I_1	Bridge output current	$1.004e^{j0.01851}$
I_C	Filter capacitor current	$0.01907e^{j1.347}$
V_{DC}	Inverter DC input voltage	0.8031
I_{DC}	Inverter DC input current	1.253

Table 2. Table of parameters used for inverter model simulation.

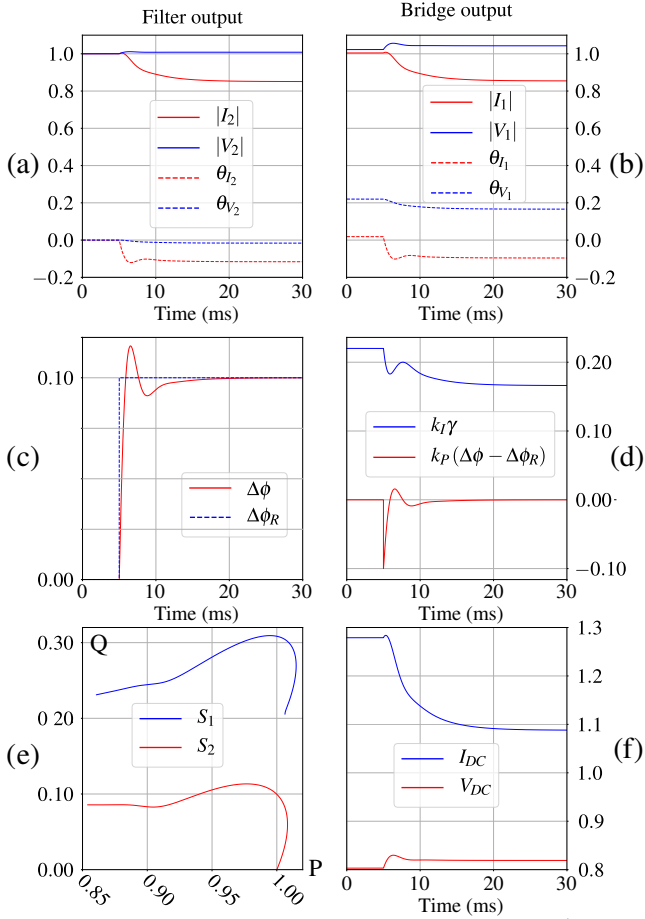|	Base values	
V_b	$110\sqrt{2}$ V	
S_b	10kVA	
Z_b	2.420Ω	
I_b	64.2824A	
	Inverter parameters	
L_1	0.11138 p.u.	
L_2	0.11138 p.u.	
C	0.02007 p.u.	
R_F	17.355 p.u.	
V_∞	$0.9950e^{j-0.10067}$ p.u.	
Z_L	$(0.01 + j0.1)$ p.u.	
τ_1	295.445 μs	
x_1	0.11138 p.u.	
τ_2	295.445 μs	
x_2	0.11138 p.u.	
κ_C	48.4ms	
y_c^0	-0.02007 p.u.	
V_S	0.928439 p.u.	
R_S	0.1 p.u.	

Figure 5. Inverter model response to a 0.10 step disturbance in power angle reference.

Initially, the system is at a unitary power factor state; when the step to power angle reference takes plate at 5ms, this new setpoint forces the inverter to supply some reactive power to the infinite bus. Figure 5.(e) shows the complex power variations involved. In order to supply some reactive power, the system needs to ramp output voltage V_2 to comply. Since the bridge output voltage is directly related to V_{DC}, this means current I_{DC} must be reduced because of the equivalent series resistance R_S of the input power source V_S. Indeed, 5.(f) shows this mechanism at work: DC current reduces, voltage rises, allowing for V_1 and V_2 to rise. This however means that the input DC current must fall, since the input voltage is higher the lower this current is due to the series resistance of the input source. However, this causes output active power to dwindle because the output current is also reduced.

Also predictably, the system reaches a new equilibrium in approximately 25 miliseconds, which is an expected result for a system comprised of fast electronic converters with low inductances. It is interesting to note that this behavior is expressed in the very low time constants involved — τ_1, τ_2 and κ.

Finally, 5.(c) and 5.(d) show the PI controller in action, adjusting the control variables to achieve the desired power angle. This control effect is also seen in 5.(e) and 5.(e), by observing that, at initial time, θ_{I_2} and θ_{V_2} are both zero and, once diturbance is applied and the PI control

takes action, the current begins lagging with respect to the voltage

The model, then, accomplishes its intended purpose: a per-unit modelling of a grid-connected inverter which yields state variables in the direct-quadrature axis.

This allows implementation of this model in mixed grids where such inverter systems coexist with classical synchronous machine models.

5. CONCLUSION AND FURTHER ADVANCEMENTS

This paper presented the Dynamic Phasor modelling applied to an inverter topology. Such technique is thoroughly explained and developed, showing mathematical results that this technique is valid for Electric Power System studies. The modelling hypotheses are explained and listed, so as to make the model comprehensive and completely understood. In this regard, the technique allows for expansion of the modelling, including lossy components like inductances winding resistances and capacitances parasitic inductances and resistances. Also, the switching losses in the electronic switches can be included to make the model more comprehensive.

Also, since a particular topology was adopted to make a case study, natural next steps are to adopt other topologies of switching bridges and filters so as to compare performance of the many topologies and how they interact with the grid.

Ultimately, the developed model is compatible with the standard modelling for Electric Power System stability studies: it presents a phasorial equivalent nature while modelling quantities in a per-unit base, enabling it to be integrated with clasically simulation programs and algorithms that use Synchronous Machine phasorial equivalent models for stability analyses.

REFERENCES

Kahlane, A.E.W.H., Hassaine, L., and Kherchi, M. (2014). LCL filter design for photovoltaic grid connected systems. *Third international seminar on new and renewable energies*, 8(2), 227–232.

Kotian, S.M. and Shubhanga, K.N. (2016). Dynamic phasor modelling and simulation. *12th IEEE International Conference Electronics, Energy, Environment, Communication, Computer, Control: (E3-C3), INDICON 2015*, 4(2), 1–6. doi:10.1109/INDICON.2015.7443446.

Kulasza, M.A. (2014). *Generalized dynamic phasor-based simulation for power systems*. Doctorate thesis, University of Manitoba.

Sanders, S.R., Noworolski, J.M., Liu, X.Z., and Verghese, G.C. (1991). Generalized Averaging Method for Power. *IEEE Trans. Power Electron.*, 6(2), 251–259.

Wu, W., Zhang, C., Su, J., and Wang, H. (2016). The Design of New High Efficiency Photovoltaic Grid and Independent Power Supply Inverter. *Proceedings - 2015 International Conference on Computational Intelligence and Communication Networks, CICN 2015*, 1579–1582. doi:10.1109/CICN.2015.300.

Zayed, A. (2008). On the Notion of Bandlimitedness and its Generalizations. *Revista de la Unión Matemática Argentina*, 49(1), 99–109.